Preparation of YAG:Ce Nanoparticles by Laser Ablation in Liquid and Demonstration of White Light Emitting Diode

Kenichi Watanabe and Hiroyuki Wada*

Institute of Science Tokyo, 4259 Nagatsuta, Migori-ku, Yokohama, Kanagawa 226-8503, Japan
**Corresponding author's e-mail: wada.h.ac@m.titech.ac.jp*

YAG:Ce nanoparticles were successfully prepared by laser ablation in liquid, and white light emitting diode (LED) with them was demonstrated. Laser (Nd:YAG, second harmonic generation (SHG), 13 ns, 532 nm, 10 Hz) was used to prepare the nanoparticles. X-ray diffraction showed that the nanoparticles were YAG:Ce, and no byproducts were produced . Pellet as raw material was minitualized by laser irradiation, and the primary particle size decreased as the laser fluence increased, producing nanoparticles with a primary size of 30 nm. The excitation spectrum of YAG:Ce nanoparticles had peaks around 339 nm and 457 nm, and the fluorescence spectrum had a broad peak between 528 and 540 nm. The blue emission from white LED was increased because scattering optical losses decreased.
DOI: 10.2961/ilmn.2025.02.2009

Keywords: laser process, phosphor, white LED, garnet, rare earth

1. Introduction

Nanoparticles are useful for applications in various areas such as catalysts, biomaterials, and electronic materials because nanoparticles have an extremely large specific surface area and exhibit properties different from those of the bulk. In general, nanoparticles are prepared by solid-phase reaction methods [1], sol-gel methods [2], and so on. The laser ablation in liquid [3-13] has attracted attention in recent years as a relatively new nanoparticle preparation method. Nanoparticles are able to be prepared by laser ablation in liquid using various compounds and liquids as raw materials, and several nanoparticle formation mechanisms and their applications were introduced in detail by D. Zhang et al [14].

Laser ablation in liquid is a method to produce nanoparticles by irradiating a target material in a liquid with a pulsed laser and then miniaturizing it. The principle of nanoparticle production by laser ablation in liquid is that laser irradiation of the target material creates a plasma of the target material, which is then rapidly cooled by the solvent surrounding the plasma to form clusters, after which nanoparticles are produced [15-17]. The characteristics of laser ablation in liquid include the following. Nanoparticles with high crystallinity can be obtained due to the high temperature and pressure conditions [18]. The collection rate is high because all the prepared nanoparticles are present in the liquid. The prepared nanoparticles are obtained as colloids, making them easy to handle. The size and shape of the nanoparticles can be controlled by changing the laser conditions [19,20]. Aggregation and dispersion can be controlled by adding surfactants to the solvent [5].

Light Emitting Diode (LED) is a device that emits light when an electric current is applied, and is widely used in traffic signals, automobile headlights, electric billboards, outdoor displays, and other applications. Compared to conventional light sources, LEDs have features such as long life and low power consumption that place a low burden on the environment. White LEDs [21] are made by placing a yellow phosphor in front of a blue LED [22] to achieve white color with blue and yellow. The best known yellow phosphor to combine with blue LEDs when fabricating white LEDs is YAG:Ce ($Y_3Al_5O_{12}$:Ce) [23]. Ce-doped YAG (Yttrium Aluminum Garnet) is an oxide, and a part of the crystal site of Y is replaced with Ce [23]. The advantages of YAG:Ce are low production cost and high luminous efficiency, and it is used as a phosphor material for lighting, bio-imaging, scintillators, etc. [23].

YAG:Ce nanoparticles were tried to be used for white LED [24]. Because blue light from blue LEDs passes through the yellow phosphor particles to reach the human eye, the intensity of blue light is likely to be reduced by light scattering loss at the yellow phosphor particles [24]. The light scattering loss can be decreased by the decrease in particle size of yellow phosphor as shown in equation (1) [25],

$$I_s = \frac{8\pi^4 N_m \alpha^6}{\lambda^4 r^2} \left|\frac{m^2-1}{m^2+2}\right|^2 (1+cos^2\theta) I_i, \quad (1)$$

where I_s is Rayleigh scattering intensity of one particle, I_i is intensity of incident light, N_m is refractive index of the medium, α is particle diameter, N_p is refractive index of the particle, $m = N_p/N_m$ is relative refractive index, λ is wavelength of incident light, r is distance between observation point and particle, and θ is scattering angle [25]. Since the scattering intensity is proportional to the sixth power of the particle diameter, the scattered light can be suppressed by the usage of YAG:Ce nanoparticles.

In this study, YAG:Ce nanoparticles are prepared by a laser ablation method in liquid and characterized. White LEDs are demonstrated by using these nanoparticles in combination with blue LEDs and their luminescence properties are evaluated.

2. Experimental methods

YAG:Ce powder (YAG C28P-KBYA-24, Tokyo Chemical Laboratory Co. 0.80 g) was added to aqueous solution of polyvinyl alcohol (Molecular weight: 2000, 5 wt%, 40 μL). The mixture was filled into a tablet mold (PT-10, Japan Spectroscopy Co.) and pressed using a hydraulic press (3.84

t) for 10 minutes to produce pellets. The pellets were sintered in a tube furnace. The sintering conditions were as follows: the temperature was raised to 800°C, kept at 800°C for 2 hours and 40 minutes, then raised to 1550°C, kept at 1550°C for 8 hours, and cooled to room temperature. To prevent oxidation from Ce^{3+} to Ce^{4+} during sintering, the electric furnace was kept under a nitrogen atmosphere.

Pellets and ultrapure water (30 ml) were added to a glass cell, and laser beam (SL8585G, Spectron Laser Systems, wavelength: 532 nm, pulse width: 13 ns, repetition frequency: 10 Hz) was irradiated to the top of the pellet for 10 minutes to obtain nanoparticles.

The crystal structure of the nanoparticles was investigated by X-ray diffraction (XRD). The nanoparticle-dispersed aqueous solution was powdered by a freeze dry (FDU-1200, EYELA) for XRD measurement. The primary particle size was measured by scanning electron microscope (SEM, acceleration voltage: 5 kV). The samples for SEM were prepared by dropping 10 µl of nanoparticle-dispersed aqueous solution onto a copper grid with a carbon support film and allowing it to dry. Photoluminescence (PL) and Photoluminescence Excitation (PLE) spectra were measured using a fluorescence spectrophotometer.

YAG:Ce nanoparticle-dispersed films were prepared for evaluation of white LEDs. Two-component mixture type silicone encapsulant (Transparent organic material, LPS-3419A and LPS-3419B, Shin-Etsu Chemical Co.) was stirred for 10 minutes. YAG:Ce nanoparticles were added to the silicone encapsulant and remixed. For concentration-dependent evaluation, the nanoparticle concentration relative to the encapsulant was set as 0.0, 0.05, 0.1, and 0.2 g/mL, and for fluence-dependent evaluation, 0.1 g/mL. A mold was prepared with a 1 mm thick glass slide on a plastic film, and the mixture of YAG:Ce nanoparticles and silicone was poured into it with a syringe. The film (thickness: 1 mm) was prepared by the doctor-blade method, and the film was dried at 60°C for 2 hours first, then at 150°C for 4 hours using a constant-temperature dryer. The film was placed in front of a blue LED (OSB5XNE3C1S, OptoSupply, 3 W) with heat sink. Voltage (2.6 to 3.6 V) was applied by a power supply (PMC-35-2A, Kikusui Electronics Co.), and spectra were measured with a fluorescence spectrophotometer (F-7000, Hitachi High-Technologies Co.).

3. Results and discussion

Figure 1 shows the XRD patterns of the nanoparticles produced at each laser fluence. They were corresponded to $Y_3Al_5O_{12}$ garnet structure as matrix, which belongs to the cubic system of space group *Ia3d* [26]. Yttrium Aluminum Monoclinic $Y_4Al_2O_9$ (YAM), Yttrium Aluminum Hexagonal $YAlO_3$ (YAH), Yttrium Aluminum Perovskite $YAlO_3$ (YAP), the angles of the strongest peaks in XRD patterns of which were different from that of YAG, and CeO_2 could be by-products, which reduced photoluminescence [26], but they were not produced. The ionic radius of Y^{3+} is 1.02 Å, which is slightly smaller than that of Ce^{3+}, 1.14 Å, but can be substituted, and this difference in ionic radii results in the formation of a Ce level within the energy level of YAG [26]. The formation of by-products due to laser irradiation would be suppressed because the peak positions and intensity ratios of the nanoparticles in Figure 1 were almost the same as those of the raw material, and only the YAG peak was observed.

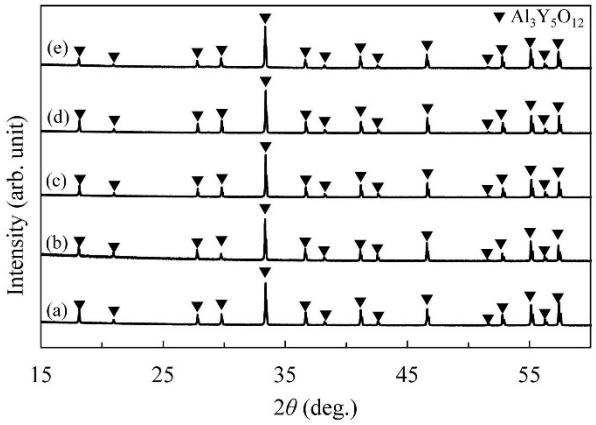

Fig. 1 XRD spectra of (a) raw material and nanoparticles at each laser fluence: (b) 1.0 J/cm^2, (c) 2.0 J/cm^2, (d) 3.7 J/cm^2 and (e) 5.0 J/cm^2.

Figure 2 shows SEM images of the raw material, and nanoparticles produced at each laser fluence. The primary particle size of the raw material consisted of particles ranging from a few µm to several tens of µm, and this average primary particle size was 21.3 µm. In contrast, the primary particle size of the nanoparticles was several tens of nm, indicating that nanoparticles were formed from the micron-size raw material by the miniaturization. As shown in Figure 3, the average primary particle size decreased with the increase in laser fluence at low laser fluences and was nearly constant at around 30 nm at high fluences above 2.0 J/cm². The aggregated fine nanoparticles at 5.0 J/cm^2 would be partially melted due to the higher laser fluence to create slightly larger nanoparticles. Hence, the average particle size and the standard deviation at 5.0 J/cm^2 were slightly increased compared to those at 3.7 J/cm^2. Two processes have been proposed for the formation of nanoparticles by laser ablation in liquids: Coulomb explosion and thermal explosion [27], and both formation mechanisms show that an increase in laser fluence leads to an increase in miniaturization. The increase in specific surface area due to miniaturization would increase the heat and other transfer from the particles to the solvent, making it more difficult for the particle temperature to increase and suppressing miniaturization.

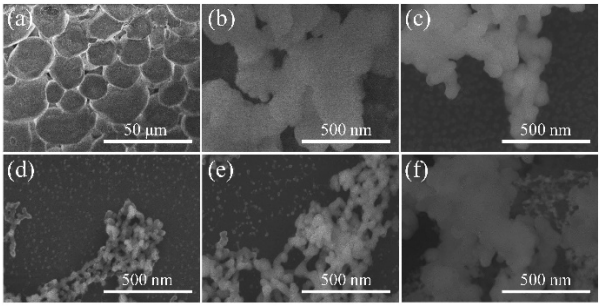

Fig. 2 SEM images of (a) raw material and nanoparticles at each fluence ((b) 0.50 J/cm^2, (c) 1.0 J/cm^2 , (d) 2.0 J/cm^2 , (e) 3.7 J/cm^2 and (f) 5.0 J/cm^2).

Figure 4 shows PL spectra of nanoparticles. YAG is transparent in visible light region, but doping with Ce produces the energy levels of Ce^{3+}, and absorption. The electron configuration of Ce^{3+} is $1s^2 2s^2 2p^6 3s^2 3p^6 3d^{10} 4s^2 4p^6 4d^{10} 4f^1 5s^2 5p^6$, and YAG:Ce emits by the transition of electron between the 4f and 5d orbitals [28,29]. Because the 4f orbital splits into $^2F_{7/2}$ and $^2F_{5/2}$, the PL spectrum has two peaks at 530 nm and 575 nm, which is observed as one broad peak [28,29].

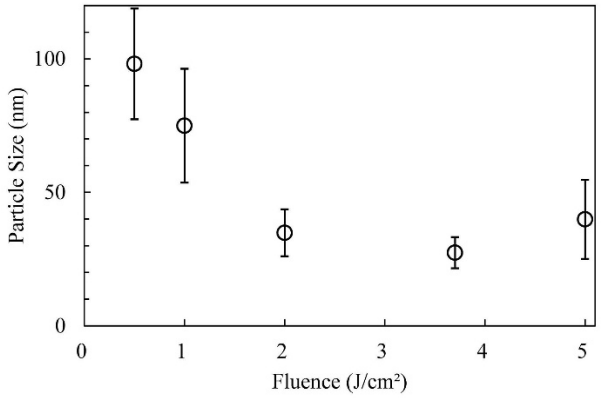

Fig. 3 The primary particle size as a function of laser fluence.

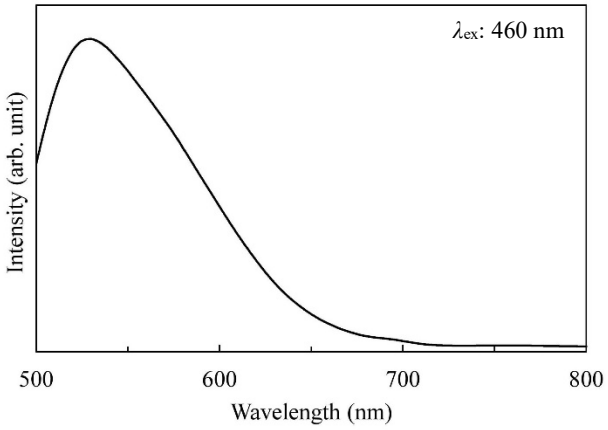

Fig. 4 PL spectrum of nanoparticles at 3.7 J/cm^2.

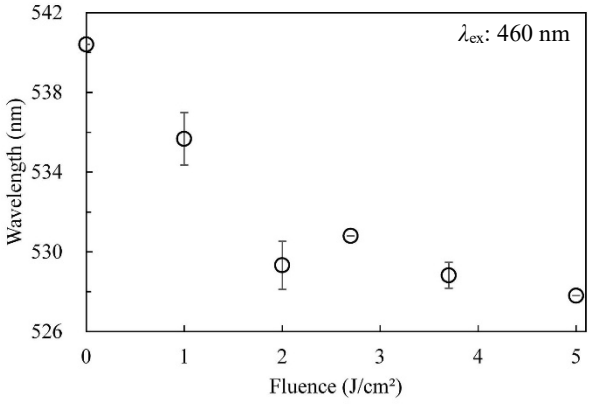

Fig. 5 Average peak wavelength of PL spectra as a function of laser fluence.

Figure 5 shows the average peak wavelengths of the PL spectra of the YAG:Ce nanoparticles. It was blue-shifted with the increase in laser fluence. There are several reports that the band gap increased when nanoparticles are formed [30-32], and this effect shortened the emission wavelength of the activator [24,33]. It was believed that this trend was observed in this study as well. When the fluence was increased above 2.0 J/cm², the average peak wavelength tended to remain constant around 529 nm.

Figure 6 shows PLE spectrum of nanoparticles. PLE had two peaks at 340 nm and 460 nm due to splitting. 4f electron is excited from the 5d orbital by light irradiation, and then emission is observed when the 5d electron returns to the 4f orbitals [28,29]. The energy difference between the absorption and emission wavelengths is called the Stokes shift ΔS, which is caused by the excited electron relaxing to the lower state while releasing energy as heat [28,29]. Figures 7(a) and (b) show the average peak wavelengths of the excitation spectra of nanoparticles. The average peak wavelengths were around 339 nm and 457 nm, which were constant and did not change when the laser fluence was changed.

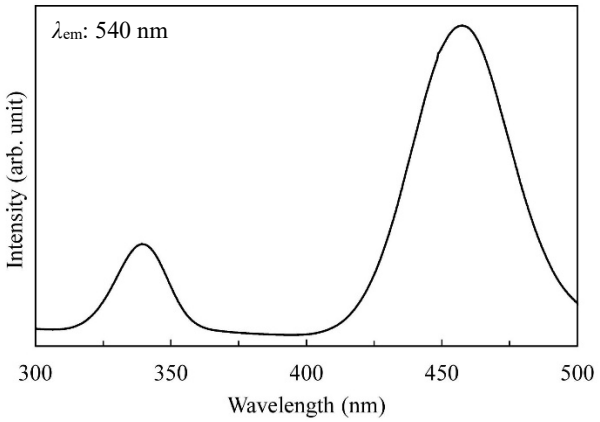

Fig. 6 PLE spectrum of nanoparticles at 3.7 J/cm^2.

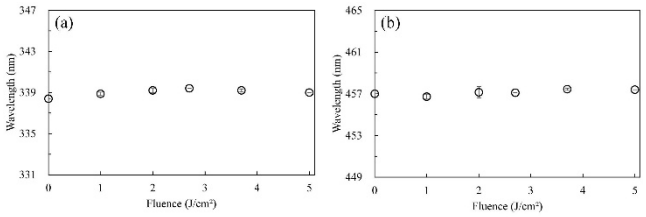

Fig. 7 Average peak wavelength of PLE spectra at (a) short and (b) long wavelength as a function of laser fluence. λ_{em}: 540 nm.

The emission spectrum of white LED fabricated by combining a YAG:Ce nanoparticle-dispersed film and a blue LED was measured. Figure 8 shows the concentration dependence of the film on the CIE 1931 chromaticity diagram. As the concentration of the YAG:Ce nanoparticle was increased, both x and y values increased and the hue changed from blue to yellow region. The point at 0.00 g/mL in the lower left was the emission of the blue LED only. The point at 0.05 g/mL had a low YAG:Ce emission intensity due to its low concentration and was still in the blue region, although it was slightly closer to the white region than the point at 0.00 g/mL. The point at 0.10 g/mL was the closest to white

in this experimental condition. The 0.20 g/mL point was in the yellow region because it contained more YAG:Ce nanoparticles than the 0.10 g/mL point. These were due to the increased proportion of broad YAG:Ce-derived peaks from 500 nm to 650 nm relative to the blue LED-derived peak near 460 nm.

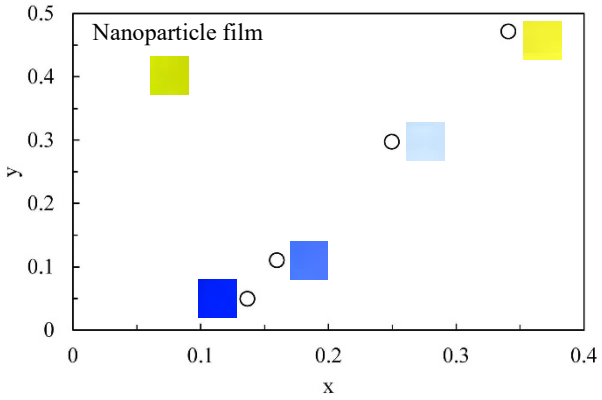

Fig. 8 x and y values of the chromaticity diagram at each concentration of YAG:Ce nanoparticles. The concentration: 0.00 g/mL, 0.05 g/mL, 0.10 g/mL, and 0.20 g/mL from bottom left to top right in the figure. Insets: Color pictures of scattering from nanoparticle film (0.10 g/m) and irradiated part of the white LED at each point.

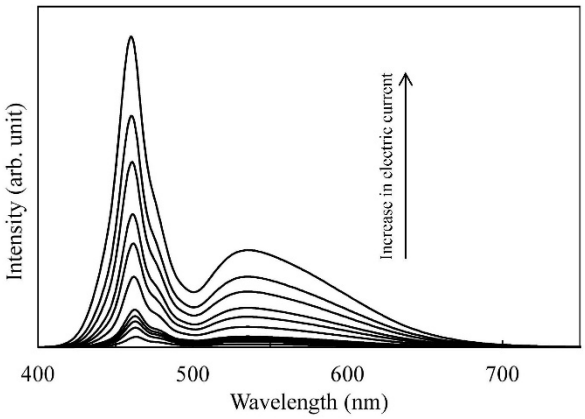

Fig. 9 Emission spectra of white LED at each electric current. The current value of the blue LED is increased from 0.01 A to 0.80 A. Concentration of YAG:Ce: 0.10 g/ml.

Figure 9 shows the emission spectrum of a white LED when the current value of the blue LED is increased from 0.01 A to 0.80 A. As the emission intensity of the blue LED increased with increasing current, that of the white LED also increased. The position of the peak wavelength did not change significantly with the change in current.

Figure 10 shows the emission spectrum of white LEDs at each laser fluence of laser ablation in liquid. Figure 11 shows the fluence dependence of the peak intensity. The highest peak intensity of blue light after passing though the yellow phosphors was obtained at 1.0 J/cm² of laser fluence. Between laser fluences of 1.0 J/cm² and 2.0 J/cm², the peak intensity around 460 nm derived from blue LEDs was larger compared to the raw material. The nanosizing of YAG:Ce raw material powder by laser ablation in liquid would decrease the scattering optical loss due to Rayleigh scattering, and then the transmitted light was increased. When the laser fluence was increased to 5.0 J/cm², the intensity of the blue LED-derived peak decreased. Figure 3 indicates the primary particle size, while the scattering intensity in Figure 10 is related to the secondary particle size, which is the total size of the aggregated particles. The peak intensity was observed at 1.0 J/cm² in Figure 11 because nanosizing more than 2.0 J/cm² would accelerate the aggregation, and then the secondary particle size would increase, which would increase the scattering. Therefore, there would be an optimal laser fluence in device fabrication.

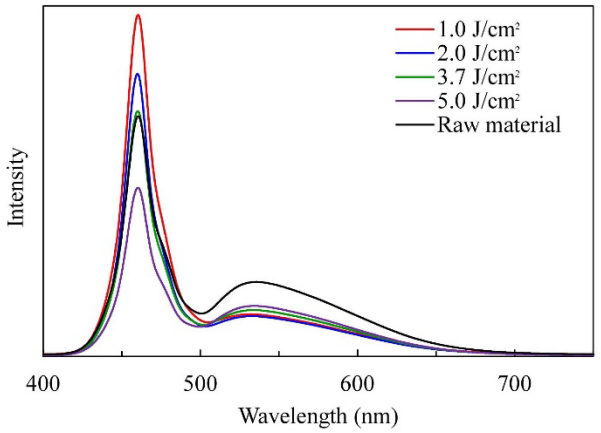

Fig. 10 Emission spectra of white LED with YAG:Ce nanoparticles at each laser fluence (Electric current: 0.40 A).

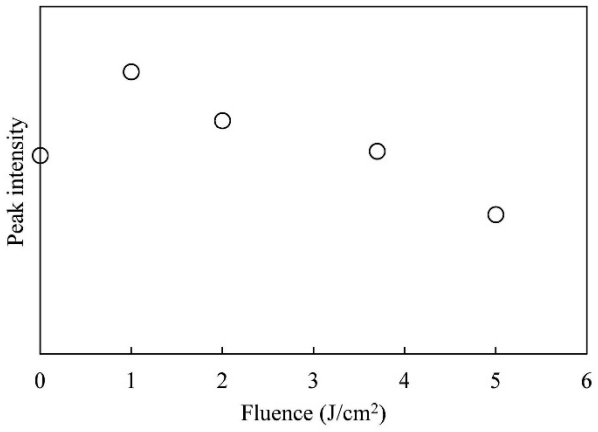

Fig. 11 Peak intensity of emission spectra of white LED with YAG:Ce nanoparticles as a function of each laser fluence (Electric current: 0.40 A).

4. Conclusions

In this study, YAG:Ce nanoparticles were successfully prepared by laser ablation in liquid and their optical properties were evaluated. The YAG:Ce nanoparticles were mixed with silicone encapsulant to form a film, which was combined with a blue LED to form a white LED, and the emission spectrum was evaluated by colorimetric calculations.

For preparation of YAG:Ce nanoparticles, no by-product was produced. The nanoparticles were miniaturized by laser irradiation. The primary particle size of the nanoparticles decreased with increasing laser fluence below 2.0 J/cm² and

remained constant at about 30 nm at fluences above 2.0 J/cm². The PL spectrum had peak wavelengths between 528 and 540 nm, and the PLE spectrum of the dispersion of the generated nanoparticles had peak wavelengths around 339 and 457 nm. With increasing laser fluence, the peak wavelength of the PL spectrum blueshifted and became constant above 2.0 J/cm². The peak wavelength of the PLE spectrum did not change with changing irradiation laser fluence.

For white LED, the transmitted light of the blue LED increased at laser fluence of 1.0 J/cm² due to the reduction of scattering optical loss by nanosizing compared to the raw material. At higher laser fluences, the blue light intensity decreased due to the increase in scattering caused by the progress of miniaturization and then the aggregation of nanoparticles.

Acknowledgments

The authors would like to thank Prof. Kitamoto for SEM, and Material Analysis Division (Suzukakedai) for XRD at Institute of Science Tokyo.

References

[1] M. A. Almessiere, N. M. Ahmed, I. Massoudi, A. L. A. Otaibi, A. A. Alshehri, and M. A. Shafouri: Optik, 158, (2018) 152.
[2] F. Selim, A. Khamehchi, D. Winarski, and S. Agarwal: Opt. Mater. Express, 6, (2016) 3704.
[3] J. Neddersen, G. Chumanov, and T. Cotton: Appl. Spectrosc., 47, (1993) 1959.
[4] A. Fojtik and A. Henglein: Ber. Bunsen Ges. Phys. Chem., 97, (1993) 252.
[5] F. Mafune, J. Y. Kohno, Y. Takeda, T. Kondow, and H. Sawabe: J. Phys. Chem. B, 104, (2000) 8333.
[6] T. Tsuji, K. Iryo, N. Watanabe, and M. Tsuji: Appl. Surf. Sci., 202, (2002) 80.
[7] C. L. Sajti, R. Sattari, B. N. Chichkov, and S. Barcikowski: J. Phys. Chem. C, 114, (2010) 2421.
[8] G. Compagnini, A. A. Scalisi, and O. Puglisi: Phys. Chem. Chem. Phys., 4, (2002) 2787.
[9] S. Salmaso, P. Caliceti, V. Amendola, M. Meneghetti, J.P. Magnusson, G. Pasparakis, and C. Alexander: J. Mater. Chem., 19, (2009) 1608.
[10] A.V. Kabashin and M. Meunier: J. Appl. Phys., 94, (2003) 7941.
[11] C. Tabor, W. Qian, and M. El-Sayed: J. Phys. Chem. C, 111, (2007) 8934.
[12] S. I. Dolgaev, A. V. Simakin, V. V. Voronov, G. A. Shafeev, and F. Bozon-Verduraz: Appl. Surf. Sci., 186, (2002) 546.
[13] N. V. Tarasenko, A. V. Butsen, and E. A. Nevar: Appl. Surf. Sci., 247, (2005) 418.
[14] D. Zhang, Z. Li, and K. Sugioka: J. Phys. Photonics, 3, (2021) 042002.
[15] D. Zhang, B. Gökce, and S. Barcikowski: Chem. Rev., 117, (2017) 3990.
[16] H. Zeng, X. W. Du, S. C. Singh, S. A. Kulinich, S. Yang, J. He, and W. Cai: Adv. Funct. Mater., 22, (2012) 1333.
[17] H. B. Zeng, W. Cai, Y. Li, J. Hu, and P. Liu: J. Phys. Chem. B, 109, (2005) 18260.
[18] W. Soliman, T. Nakano, N. Takada, and K. Sasaki: Jpn. J. Appl. Phys., 49, (2010) 116202.
[19] H. Zhang, G. Duan, Y. Li, X. Xu, Z. Dai, and W. Cai: Cryst. Growth Des., 12, (2012) 2646.
[20] F. Yoshimura, K. Nakamura, F. Wakai, M. Hara, M. Yoshimoto, O. Odawara, and H. Wada: Appl. Surf. Sci., 257, (2011) 2170.
[21] F. A. Ponce and D. P. Bour: Nature, 386, (1997) 351.
[22] S. Nakamura, M. Senoh, and T. Mukai: Jpn. J. Appl. Phys., 30, (1991) 1708.
[23] V. Bachmann, C. Ronda, and A. Meijerink: Chem. Mater., 21, (2009) 2077.
[24] R. Kasuya, A. Kawano, and T. Isobe: Appl. Phys. Lett., 91, (2007) 111916.
[25] C. F. Bohren and D. R. Huffman: "Absorption and Scattering of Light by Small Particles" (Wiley-VCH, Weinheim, 1998) p. 132.
[26] Z. Hassan, H. R. Abd, F. H. Alsultany, A. F. Omar, and N. M. Ahmed: Mater. Chem. Phys., 229, (2019) 22.
[27] S. Inasawa, M. Sugiyama, and Y. Yamaguchi: J. Phys. Chem. B, 109, (2005) 9404.
[28] Q. Li, L. Gao, and D. Yan: Mater. Chem. Phys., 64, (2000) 41.
[29] Y. S. Lin, R. S. Liu, and B.-M. Cheng: J. Electrochem. Soc., 152, (2005) J41.
[30] A. L. Efros and A. L. Efros: Sov. Phys. Semicond., 16, (1982) 772.
[31] L. E. Brus: J. Chem. Phys., 80, (1984) 4403.
[32] M. G. Bawendi, M. L. Steigerwald, and L. E. Brus: Annu. Rev. Phys. Chem., 41, (1990) 477.
[33] N. Tsuruoka, T. Sasagawa, T. Yodo, M. Yoshimoto, O. Odawara, and H. Wada: SpringerPlus, 5, (2016) 325.

(Received: June 12, 2025, Accepted: August 15, 2025)